A Section 508–conformant HTML version of this article is available at https://doi.org/10.1289/EHP1275.

Regulation of Chromatin Assembly and Cell Transformation by Formaldehyde Exposure in Human Cells

Danqi Chen,[1] Lei Fang,[1] Shenglin Mei,[2] Hongjie Li,[1†] Xia Xu,[1] Thomas L. Des Marais,[1] Kun Lu,[3] X. Shirley Liu,[4] and Chunyuan Jin[1]*

[1]Department of Environmental Medicine and Biochemistry and Molecular Pharmacology, New York University School of Medicine, New York, New York, USA
[2]Department of Bioinformatics, School of Life Sciences, Tongji University, Shanghai, China
[3]Department of Environmental Sciences and Engineering, University of North Carolina, Chapel Hill, North Carolina, USA
[4]Department of Biostatistics and Computational Biology, Dana-Farber Cancer Institute and Harvard T.H. Chan School of Public Health, Boston, Massachusetts, USA

Background: Formaldehyde (FA) is an environmental and occupational chemical carcinogen. Recent studies have shown that exogenous FA causes only a modest increase in DNA adduct formation compared with the amount of adducts formed by endogenous FA, raising the possibility that epigenetic mechanisms may contribute to FA-mediated carcinogenicity.

Objectives: We investigated the effects of FA exposure on histone modifications and chromatin assembly. We also examined the role of defective chromatin assembly in FA-mediated transcription and cell transformation.

Methods: Cellular fractionation and Western blot analysis were used to measure the levels of histone modifications in human bronchial epithelial BEAS-2B cells and human nasal RPMI2650 cells in the presence of FA. Chromatin immunoprecipitation (ChIP) and micrococcal nuclease (MNase) digest assays were performed to examine the changes in chromatin assembly and accessibility after FA exposure. RNA sequencing (RNA-seq) and real-time polymerase chain reaction (PCR) were used to examine transcriptional dysregulation. Finally, anchorage-independent cell growth ability was tested by soft agar assay following FA exposure.

Results: Exposure to FA dramatically decreased the acetylation of the N-terminal tails of cytosolic histones. These modifications are important for histone nuclear import and subsequent chromatin assembly. Histone proteins were depleted in both the chromatin fraction and at most of the genomic loci tested following FA exposure, suggesting that FA compromises chromatin assembly. Moreover, FA increased chromatin accessibility and altered the expression of hundreds of cancer-related genes. Knockdown of the histone H3.3 gene (an H3 variant), which mimics inhibition of chromatin assembly, facilitated FA-mediated anchorage-independent cell growth.

Conclusions: We propose that the inhibition of chromatin assembly represents a novel mechanism of cell transformation induced by the environmental and occupational chemical carcinogen FA. https://doi.org/10.1289/EHP1275

Introduction

Formaldehyde (FA) is widely used in the production of industrial and consumer products; therefore, FA can be detected in many households and building materials (IARC 2012; Swenberg et al. 2013). FA is also generated as a by-product of combustion. Common environmental sources include tobacco smoke, automotive exhaust fumes, and fires. In addition, FA is released from products used in building materials, such as particle board and carpet. Occupational workers in industries related to the production of resins, plastics, wood, paper, textiles, and general chemicals as well as medical professionals who use embalming products and disinfectants could be exposed to high levels of FA. Concentrations of FA for human exposure vary. In the United States, high levels of exposure to FA were reported for FA-based resin production (mean concentrations of $\leq$14.2 ppm), plastic product production ($\leq$38.2 ppm), and pathology autopsy laboratories ($\leq$4.35 ppm) (NTP 2011). Recent studies reported that industrial workers could still be exposed to several parts per million of FA. For instance, FA exposure levels ranged from 0.18 ppm to 2.37 ppm in a wood processing factory and from 0.51 ppm to 2.60 ppm in a utensil factory (Wang et al. 2015; Zhang et al. 2010b). The International Agency for Research on Cancer (IARC) classified FA as a Group 1 human carcinogen (IARC 2012). Considerable evidence links FA exposure to both human nasopharyngeal cancer (Hauptmann et al. 2004; Marsh et al. 2007; Vaughan et al. 2000) and nasal carcinoma in animals (Kerns et al. 1983; Swenberg et al. 1980). Exposure to FA has also been implicated in leukemia (Goldstein 2011; Zhang et al. 2010a).

The molecular mechanisms of FA-induced carcinogenesis are not fully understood at the present time. The accumulation of DNA damage and the resulting mutagenesis induced by DNA adducts and DNA–protein cross-links (DPCs) have been the focus of FA research (Swenberg et al. 2013). Various forms of genetic damage including DPCs, DNA cross-links, nucleotide base adducts, mutations, and micronuclei were observed in the nasal tissues of animal models and humans exposed to FA. For example, DPCs were detected in the respiratory track of rhesus monkeys exposed to FA, corresponding to the tumor sites observed in humans (Casanova et al. 1991). DNA cross-links were found to be correlated with tumor incidence in FA-exposed rats (Liteplo and Meek 2003). Rats exposed to FA developed N^2-hydroxymethyl-dG adducts (Lu et al. 2010) and p53 gene mutations at G:C base pairs at the p53 mutational hot spots found in human cancers (Recio et al. 1992). Numerous studies found an increased frequency of micronuclei in the nasal epithelium and the buccal epithelium of workers exposed to FA (NTP 2011). In

Address correspondence to C. Jin, Dept. of Environmental Medicine, New York University School of Medicine, 57 Old Forge Rd., Tuxedo Park, NY 10987 USA. Telephone: (845) 731-3602. Email: Chunyuan.jin@nyumc.org

*Current affiliation: Medical School of Nanjing University, Nanjing, China.

†Current affiliation: Dept. of Pathology, State University of New York Downstate Medical Center, Brooklyn, NY, USA.

Supplemental Material is available online (https://doi.org/10.1289/EHP1275).

The authors declare they have no actual or potential competing financial interests.

Received 25 October 2016; Revised 19 May 2017; Accepted 23 May 2017; Published 21 September 2017.

Note to readers with disabilities: *EHP* strives to ensure that all journal content is accessible to all readers. However, some figures and Supplemental Material published in *EHP* articles may not conform to 508 standards due to the complexity of the information being presented. If you need assistance accessing journal content, please contact ehponline@niehs.nih.gov. Our staff will work with you to assess and meet your accessibility needs within 3 working days.

addition, Monticello et al. showed that cellular proliferation was correlated with nasal tumor incidence in animal exposure studies (Monticello et al. 1989, 1996). Recent studies on endogenous versus exogenous FA-DNA adducts have shown that the amount of DNA adducts caused by exogenous FA exposure is only modestly increased compared with the level of adducts formed by endogenous FA (Lu et al. 2010, 2011; Moeller et al. 2011; Swenberg et al. 2011). These findings have raised questions about the role of genetic damage in FA-induced carcinogenesis and have suggested the possibility that epigenetic mechanisms may contribute to FA-mediated carcinogenicity. Epigenetic mechanisms include changes in DNA methylation, histone modifications, and microRNA (miRNA) expression. It has been reported that FA exposure can change microRNA expression profiles, which can alter the signaling pathways associated with diseases such as cancer (Rager et al. 2011, 2013).

FA is an electrophilic compound; therefore, it can form protein adducts by reacting with the nucleophilic side chains of amino acids such as lysine. The reaction between lysine residues and FA generates the intermediate N^6-hydroxymethyl-lysine, from which a labile Schiff base or the more stable N^6-formyllysine can be produced by subsequent dehydration or oxidation reactions, respectively (Figure 1A). Jiang et al. first demonstrated the presence of N^6-formyllysine residues in several sources of histone proteins to the extent of 0.04–0.1% of all lysines in acid-soluble chromatin proteins (Jiang et al. 2007). Sites of N^6-formylation of lysines in histones isolated from cultured cells and from human and mouse tissues were characterized at residues involved in the regulation of chromatin function (Wiśniewski et al. 2008). Later, it was discovered that FA is the major source of N^6-formyllysine (Edrissi et al. 2013a). Moreover, the levels of N^6-formyllysine in histone proteins were increased in a dose-dependent manner in cells as well as in the nasal epithelium of rats exposed to FA (Edrissi et al. 2013a, 2013b). Interestingly, N^6-formyllysine residues were found to be refractory to acetylation in cells and *in vitro* (Edrissi et al. 2013a), as observed with FA-induced Schiff bases on lysine residues in histone H4 peptide (Lu et al. 2008). Because both Schiff bases and N^6-formyllysine are resistant to physiological modifications (Edrissi et al. 2013a; Lu et al. 2008), it has been proposed that FA–histone lysine adducts interfere with chromatin function and increase the potential for carcinogenesis (Galligan and Marnett 2017).

Histone posttranslational modifications (PTMs) are crucial for most DNA-templated processes including transcription, DNA repair, and replication (Kouzarides 2007). Histone PTMs also play important roles in histone nuclear import and chromatin assembly (Burgess and Zhang 2013; Ejlassi-Lassallette et al. 2011; Ejlassi-Lassallette and Thiriet 2012). The lysine (K) residues K5 and K12 on most newly synthesized cytosolic histones type H4 are acetylated (Burgess and Zhang 2013). These modifications, highly conserved across species, are required for histone deposition. They regulate the interaction between H3/H4 and Importin-4, a nuclear transport receptor, in addition to the well-knownhistone chaperone anti-silencing function 1 (ASF1). In yeast, acetylation of five lysine residues on H3 (K9, K14, K18, K23, and K27) facilitates chromatin assembly (Burgess et al. 2010). In *Drosophila*, aberrant truncation of the N-terminal tail of H3 compromised replication-coupled nucleosome assembly, suggesting that the role of acetylation of the N-terminal tail of histone H3 might be conserved across different species (Ahmad and Henikoff 2002). Moreover, H3K56 acetylation is important for nucleosome assembly during DNA replication and repair, in both budding yeast and humans, by enhancing the interaction between H3 and chromatin assembly factor-1 (CAF-1) (Burgess and Zhang 2013).

Here, we show that FA readily forms adducts with histones in cells and dramatically decreases lysine acetylation of the cytosolic histones H3 and H4. These acetylation modifications are critical for histone nuclear import and chromatin assembly. The transport of histone H3 into chromatin is compromised following FA exposure, resulting in changes in chromatin accessibility and in subsequent gene transcription. Interestingly, a number of tumor suppressor genes and oncogenes that are related to head and neck cancer and/or to hematological neoplasia are identified as FA-responsive genes mediated by blocking chromatin assembly. Moreover, inhibition of chromatin assembly facilitates anchorage-independent growth of cells. These data suggest that compromising chromatin assembly through inhibition of lysine acetylation on newly synthesized histones represents a possible new mechanism underlying FA-induced carcinogenesis.

Methods

Cell Culture and Treatment

The immortalized human bronchial epithelial cell line BEAS-2B and the human osteosarcoma cell line UTA6 were maintained in Dulbecco's modified Eagle medium (DMEM) supplemented with 10% fetal bovine serum (FBS), 100 U/mL penicillin, and 100 μg/mL streptomycin. The human nasal septum quasidiploid tumor cell line RPMI2650 was maintained in Eagle's minimal essential medium (EMEM) with 2 mM glutamine, 1% nonessential amino acids, 10% FBS, 100 U/mL penicillin, and 100 μg/mL streptomycin. Cells were incubated at 37°C in a humidified atmosphere of 5% carbon dioxide. In all experiments, cells (1×10^7) were seeded into 15-cm dishes with growth medium and were allowed to reach 60% confluence before exposure to FA. Doses of FA ranged from 0 to 0.5 mM for 6 h. For chronic FA exposure, cells were treated with 0 to 0.1 mM FA for 96 h. BEAS-2B cells express the epithelium marker cytokeratin 7 (CK7), although here, they were grown in DMEM instead of the recommended keratinocyte growth medium (KGM) (see Figure S1).

Cell Transfection

Transfections were carried out using Lipofectamine 2000 (Invitrogen) according to the manufacturer's instructions. Control short interfering RNA (siRNA) or two distinct siRNAs for H3.3 (H3.3 siRNA1 and H3.3 siRNA 2) (Sigma) were transfected into BEAS-2B cells to knock down H3.3 expression. For H3.3 overexpression, the pcDNA3.1-FLAG-H3.3 plasmid was transfected into BEAS-2B cells. pcDNA3.1 empty vector was used as the control.

Antibodies

Anti-histone H3 (ab1791), antiacetyl-histone H4 Lys-12 (ab61238), and anti-β-actin (ab8226) were purchased from Abcam; anti-dinitrophenyl (DNP; D9656), which reacts with DNP–bovine serum albumin (BSA) and DNP–rabbit serum albumin but not with BSA or rabbit serum albumin, was purchased from Sigma-Aldrich; antiacetyl-histone H3 (06-599), anti-trimethyl-histone H3 Lys-4 (07-473), anti-dimethyl-histone H3 Lys-9 (07-441), anti-trimethyl-histone H3 Lys-27 (07-499), antiacetyl-histone H3 Lys-18 (07-354), and anti-histone H4 (07-108) were purchased from Millipore; and anticaspase-3 (CST9662) was purchased from Cell Signaling Technology.

Trypan Blue Staining and Cell Viability Assay

Postexposure, cells were trypsinized, centrifuged, and resuspended in DMEM culture medium. The total number of viable cells was determined by trypan blue staining. Cell viability was assessed by

calculating the percentage of live cells within five randomly selected fields. Independent experiments were repeated three times.

Soft-Agar Assays

After transfection and FA treatment, cells were seeded in soft agar growth medium in 6-well plates (5,000 cells/well) and incubated at 37°C for 4–5 wk. Colonies were stained with INT/BCIP (Roche) and photographed. Colonies larger than 50 μm were counted. Independent experiments were performed three times. The results are presented as ± fold change.

Cell Lysates, Acid Extraction, and Western Blot Analysis

After FA exposure, cells were washed with ice-cold phosphate-buffered saline (PBS) and collected by centrifugation. Whole-cell lysates were prepared using Triton X-100 lysis buffer [pH 7.4; 50 mM Tris-HCl, 1% Triton X-100, 0.5% sodium deoxycholate, 0.1% sodium dodecyl sulfate (SDS), 500 mM sodium chloride (NaCl), 10 mM magnesium chloride ($MgCl_2$), 10 mM sodium butyrate, protease inhibitors]. For acid extraction, cells were resuspended in lysis buffer (pH 7.5; 10 mM HEPES, 1.5 mM $MgCl_2$, 10 mM potassium chloride (KCl), 0.2 M hydrochloric acid (HCl), 0.5 mM dithiothreitol (DTT), 10 mM sodium butyrate, and protease inhibitors], incubated on ice for 60 min, and centrifuged at 11,000 × g for 10 min. The supernatant was collected and neutralized using one-fifth volume of 1.5 M Tris-HCl buffer (pH 8.8). Total protein (50 μg) was separated on 14% polyacrylamide gel by electrophoresis and transferred to a polyvinylidene difluoride (PVDF) membrane (Bio-Rad). The membrane was cut according to the predicted size of the target proteins. Nonspecific binding was blocked by incubation in Tris-buffered saline (TBS) containing 0.1% TWEEN®-20 and 5% dry nonfat milk. Immunoblotting was performed with primary antibodies overnight at 4°C, followed by incubation with a peroxidase-conjugated second antibody. The reagent for enhanced chemiluminescence (Bio-Rad) was used for detection and developed on X-ray film. Independent experiments were performed three times.

Cellular Fractionation

Cells (4×10^7) were suspended in 1.5 mL of hypotonic buffer (pH 7.4; 10 mM Tris-HCl, 10 mM KCl, 1.5 mM $MgCl_2$, 1 mM DTT, and protease inhibitors) for 10 min on ice and centrifuged at 2,500 × g for 10 min after disruption through a 25-gauge needle. The supernatant was retained as the cytosolic fraction. The remaining pellet was resuspended in 0.5 pellet volume of low-salt buffer [pH 7.4; 20 mM Tris-HCl, 20 mM KCl, 1.5 mM $MgCl_2$, 1 mM DTT, 0.2 mM ethylenediaminetetraacetic acid (EDTA), 25% glycerol, and protease inhibitors] and homogenized using a 25-gauge needle. The sample volume was carefully measured, and 0.5 vol of high-salt buffer (pH 7.4; 20 mM Tris-HCl, 1.2 M KCl, 1.5 mM $MgCl_2$, 1 mM DTT, 0.2 mM EDTA, 25% glycerol, and protease inhibitors) was added to obtain a final KCl concentration of 0.42 M. Samples were incubated on a rotator for 30 min at 4°C; then, the suspension was centrifuged at 14,000 × g for 15 min, and the supernatant was retained as nuclear extract. The insoluble pellet was resuspended in Tris buffer [pH 7.4; 10 mM Tris-HCl, 10 mM sodium chloride (NaCl), 3 mM $MgCl_2$, and protease inhibitors] containing 1.5 mM calcium chloride ($CaCl_2$). The sample was disrupted by four passes through a 20-gauge needle and another four passes through a 25-gauge needle. The suspension was then adjusted until the amount of nucleic acid in 1 mL of the sample had an optical density of 100 ($A_{260} = 100$) and digested with 12×10^{-2} units/μL micrococcal nuclease (MNase) for 12 min at 37°C. The reaction was terminated by the addition of EDTA (10 mM, final concentration). The suspensions were then incubated on ice for 30 min. After incubation, the supernatant was collected as the S1 subfraction. The remaining pellet was resuspended in the Tris buffer plus 0.25 mM EDTA, incubated on ice for 15 min, and passed four times through a 25-gauge needle. After centrifugation at 14,000 × g for 10 min, the supernatant was collected as the S2 fraction and combined with S1 as the chromatin fraction.

Histone Carbonyl Assays

Histone carbonyl assays were performed as described by Thompson and Burcham (2008), using 15 μg of acid-extracted total histones as substrates.

Nucleosome Preparation and Chromatin Immunoprecipitation

Mono- and dinucleosomes were isolated by MNase digestion and sucrose gradient purification. Chromatin immunoprecipitation (ChIP) analysis was performed as described previously (Jin and Felsenfeld 2006). See Table 1 for primers.

MNase Digestion Assay

Nuclei were isolated from FA-treated and control BEAS-2B cells as described previously (Jin and Felsenfeld 2006). The A_{260} of the suspension was adjusted to 1.25. For the digestion, MNase was added (3×10^{-3}, 6×10^{-3}, 12×10^{-3}, or 24×10^{-3} units/μL, final concentration), and the suspension was incubated for 10 min at 37°C. The reaction was stopped by the addition of EDTA to a final concentration of 10 mM. Proteinase K (1%, v/v) and SDS (1%, w/v) were also added, and the mixture was incubated overnight at 37°C. The DNA was purified by phenol/chloroform extraction and ethanol precipitation. Purified DNA (3 μg) was separated on a 2% agarose gel and visualized by ethidium bromide staining. Independent experiments were performed three times.

MNase–Real-Time Quantitative Polymerase Chain Reaction to Determine Nucleosome Occupancy

Nuclei were prepared from FA-treated and untreated cells and were treated with different concentrations of MNase. Mononucleosomes were prepared and purified on a 5–30% sucrose gradient as described previously (Jin and Felsenfeld 2007). DNA fragments from MNase-digested nucleosomes were purified by phenol/chloroform extraction and ethanol precipitation and were quantified

Table 1. The primers used for chromatin immunoprecipitation (ChIP) analysis.

Gene ID	Forward primer	Reverse primer
EGR-2 (early growth response-2)	5′-CAGCGACGTCACGGGTATT-3′	5′-CGCCGAGCTATTAATCAATTGC-3′
IAP (inhibitor of apoptosis)	5′-CCGCTGGAGTTCCCCTAAG-3′	5′-CGCACTCCTCCCAGTGGTT-3′
S100A10	5′-GCAGGGTCATCCAGCAAGTAA-3′	5′-GCGCAGAACCAGAGAAGCGAAGAA-3′
MT1F	5′-TCCTGCAAGTGCAAAGAGTC-3′	5′-AAAGGTTGTCCTGGCATCAG-3′
H3.3B	5′-ACGAAAGCCGCCAGGAA-3′	5′-CTGTAGCGATGAGGCTTCTTCA-3′
GAPDH body	5′-AGGCTGTGGGCAAGGTCAT-3′	5′-CAGGTCCACCACTGACACGTT-3′
OSTF1	5′-TGTACTCATGGTGGCGTGGTG-3′	5′-GGCGGGCAGTAGGTCATC-3′
SAT2	5′-TGAATGGAATCGTCATCGAA-3′	5′-CCATTCGATAATTCCGCTTG-3′

using a PicoGreen fluorescence kit (Molecular Probes). The same amount of DNA in each sample was used in real-time quantitative polymerase chain reaction (qPCR) to determine the differences in the abundance of specific target DNA sequences obtained from untreated cells and from cells treated with FA. If a genomic locus is occupied by nucleosomes in untreated cells, the corresponding DNA fragment will be protected from the MNase treatment and can easily be amplified by qPCR. However, if nucleosome occupancy of the region is reduced following FA exposure, the DNA fragment is largely removed by MNase digestion and cannot be properly amplified. Accordingly, the ratio of the concentration of a target sequence protected from MNase digestion in FA-treated cells versus that in untreated cells will be <1.

RNA Sequencing

Total RNA from FA-treated BEAS-2B cells was converted into complementary DNA (cDNA) libraries using a Truseq RNA Sample Preparation V2 Kit (Illumina). Validation of library preparations was performed on an Agilent Bioanalyzer using the DNA1000 kit. Library concentrations were adjusted to 4 nM, and libraries were pooled for multiplex sequencing. Pooled libraries were denatured and diluted to 15 pM and then clonally clustered onto the sequencing flow cell using the Illumina cBOT Cluster Generation Station and a TruSeq Paired-End Cluster Kit v3-cBot-HS. Sequencing was performed on an Illumina HiSeq2500 Sequencing System using a TruSeq SBS Kit v3-HS. Quality control of FASTQ data was performed using FastQC (version 0.10.1; Babraham Bioinformatics group), and RNA reads were mapped to the human genome (UCSC hg19; February 2009 release; Genome Reference Consortium GRCh37) using STAR (version 2.5.2; Alexander Dobin) (Dobin et al. 2013) with the human reference GTF annotation file (GRCh37). Transcript counts were calculated and normalized using Gfold (version 1.0.8; Jianxing Feng) and DESeq (version 1.6.1; Simon Anders) (Anders and Huber 2010; Feng et al. 2012). The DESeq negative binomial distribution was used to call differentially expressed genes. A total of 654 genes were identified as differentially expressed genes ($p < 0.05$). Differentially expressed genes were further investigated for biological function and pathway enrichment using Ingenuity Pathway Analysis (IPA, Qiagen). RNA-seq data have been deposited in the Gene Expression Omnibus database (accession number GSE87541).

RNA Extraction and Real Time Quantitative RT-PCR

Total RNA was extracted using TRIzol reagent (Invitrogen) according to the manufacturer's protocol. The quantity and purity of the RNA prepared from each sample were determined by UV absorbance spectroscopy. Reverse transcription (RT) was performed using the SuperScript III First-Strand Synthesis System (Invitrogen) with 1 μg of RNA in a final reaction volume of 20 μL. After incubation at 50°C for 50 min, RT was terminated by heating at 85°C for 5 min. Quantitative real-time PCR analysis was performed using Power SYBR Green PCR Master Mix (Applied Biosystems). PCR was performed in triplicate. Transcripts of target genes were calculated with the ΔΔCt method using the formula $R = 2^{-\Delta\Delta Ct}$, where R is the relative expression ratio of a target gene in comparison to a reference gene, and $\Delta\Delta Ct = \Delta Ct(\text{target}) - \Delta Ct(\text{reference})$. ΔCt (target) is the Ct deviation of untreated – treated sample of the target gene transcript; ΔCt (reference) is the Ct deviation of untreated – treated sample of the reference gene transcript. In this method, the relative levels of the target gene expression are presented as a fold change relative to the reference gene expression. A relative quantity of 1 indicates no change in expression levels. For the ΔΔCt method to be valid, the PCR efficiencies of the target and the reference must be approximately equal. Thus, we assessed the efficiencies of the target amplifications and the reference (Tubulin) amplification using the equation $E = 10^{[-1/\text{slope}]}$ as described by Pfaffl (2001). The real-time PCR efficiency of Tubulin amplification was 2.18, and the efficiencies of most of the target genes we tested were between 2.14 and 2.21. For these genes, we used the ΔΔCt method to calculate their relative gene expressions given that the efficiencies were approximately equal. However, we analyzed the data for the genes *HMGA2, SERPINB5, MYEOV, HES1*, and *LAMA4* using the Pfaffl method (Pfaffl 2001) because the amplication efficiencies of these genes were between 1.54 and 1.99. See Table 2 for primers.

Statistical Analysis

Gel intensities were quantified using ImageJ (version 1.46r; National Institutes of Health) image processing software. Relevant results are presented as the mean ± standard deviation (SD) (error bars). Sig-nificance was assessed using Student's *t*-test ($p < 0.05$). Rep-licates of experiments are indicated in the figure legends.

Results

FA Adducts with Histone Proteins in BEAS-2B Cells

Given that FA exposure occurs mainly by inhalation, nontransformed human bronchial epithelial BEAS-2B cells were used as the experimental model for this study. According to the concentrations of FA for human expsoure, 1–15 ppm FA has been

Table 2. The primers used for real-time quantitative RT-PCR analysis.

Gene ID	Forward primer	Reverse primer
HES1	5′-ACGACACCGGATAAACCAAA-3′	5′-CGGAGGTGCTTCACTGTCAT-3′
FOS	5′-CCAACCTGCTGAAGGAGAAG-3′	5′-AGATCAAGGGAAGCCACAGA-3′
EGR1	5′-AGCCCTACGAGCACCTGA-3′	5′-GGCAGTCGAGTGGTTTGG-3′
DUSP1	5′-CCTGTGGAGGACAACCACAAG-3′	5′-GCCTGGCAGTGGACAAACA-3′
LAMA4	5′-GTAATGCCTACTTTACCAGGGT-3′	5′-GGGAGTTTCAGAGCAACAGG-3′
JUN	5′-CGGAGAGGAAGCGCATGA-3′	5′-TTCTCTCCAGCTTCCTTTTTCG-3′
JUNB	5′-GCTCGGTTTCAGGAGTTTGT-3′	5′-ATACACAGCTACGGGATACGG-3′
CDH1	5′-CATTGCCACATACACTCTCTTCT-3′	5′-CGGTTACCGTGATCAAAATCTC-3′
CDKN1A	5′-CCTGGAGACTCTCAGGGTCG-3′	5′-GCGTTTGGAGTGGTAGAAAT-3′
MMP3	5′-GGGTGAGGACACCAGCATGA-3′	5′-CAGAGTGTCGGAGTCCAGCTTC-3′
CSF2	5′-GGGAGCATGTGAATGCCATC-3′	5′-GGCTCCTGGAGGTCAAACAT-3′
CCND1	5′-GCGTCCATGCGGAAGATC-3′	5′-ATGGCCAGCGGGAAGAC-3′
HMGA2	5′-AAGTTGTTCAGAAGAAGCCTGCTCA-3′	5′-TGGAAAGACCATGGCAATACAGAAT-3′
SERPIN	5′-CAGAGTCAACAAGACAGACACCAA-3′	5′-CATACAGAACGTGGCCTCCAT-3′
NYEOV	5′-CCTAAATCCAGCCACGTCAT-3′	5′-GACACACCACGGAGACAATG-3′
MMP1	5′-TGGACCTGGAGGAAATCTTG-3′	5′-AGAATGGCCGAGTTCATGAG-3′
Tubulin	5′-CGGCTGAATGACAGGTATCCTAAG-3′	5′-CTCGTCCTGGTTGGGAAACA-3′

routinely used for *in vivo* studies. Because the 0.5 mM dose is equivalent to 15 ppm, to determine suitable FA concentrations to be used, we measured cell viability using conventional trypan blue viability assays with BEAS-2B cells upon exposure to either 0.25 mM or 0.5 mM FA (Figure 1B). The results show >90% cell viability for 6 h of treatment (Figure 1B). Subcytotoxic doses (>80% cell viability) were considered to give meaningful outcomes in *in vitro* toxicogenomics studies, such as those that examine carcinogenesis (Mathijs et al. 2010; van Kesteren et al. 2011). No signs of apoptosis were observed when cells were treated with up to 1 mM FA for 6 h (Figure 1C). Based on these results, it was determined that cells would be treated with 0.5 mM FA for 6 h.

Protein carbonyl assays were utilized to determine whether FA forms adducts with histone proteins in BEAS-2B cells (Suzuki et al. 2010; Thompson and Burcham 2008). Because aldehydes react with proteins to form carbonyl-retaining adducts, carbonylated protein is a highly sensitive indicator of protein adduction. Total histones were prepared by acid extraction. Figure 1D shows bands corresponding to core histones. Total histones were then incubated with a solution of 0.5% 2,4-dinitrophenyl hydrazine (DNPH) (w/v) in 10% trifluoroacetic acid (v/v). After carbonyl derivatization, carbonylated proteins were detected by Western blot analysis. The results of histone carbonylation assays suggest that FA reacts with proteins. The carbonylated protein bands partially overlapped with the H3 bands when the same membrane was reprobed with anti-histone H3 (Figure 1E), suggesting that FA forms adducts with histone proteins in BEAS-2B cells.

Effects of FA on Acetylation of the N-Terminal Tails of Cytosolic Histones

The formation of FA-histone adducts on lysine residues prevents the acetylation of the same site by histone acetyltransferase (HAT) (Lu et al. 2008; Rager et al. 2013). Given that FA reacts with histones in BEAS-2B cells (Figure 1), we hypothesized that FA may inhibit the induction of physiologic PTMs on histone proteins. To test this hypothesis, total histones were isolated by acid extraction from BEAS-2B cells treated with or without FA. Histone PTMs were detected by Western blot analysis. Unexpectedly, no significant alterations were observed (Figure 2A). The previous observation that FA cannot react with acetylated sites on histones (Lu et al. 2008) suggests that FA likely reacts with unmodified, newly synthesized histones. Because such histones localize to the cytoplasm and represent only a small percentage of total histones (Loyola et al. 2006), this change may not be detectable when total histones are analyzed. To confirm this possibility, the cytosolic fraction (the water-soluble components of cytoplasm), the nuclear extract, and soluble chromatin fractions were isolated as previously described (Chen et al. 2013) and analyzed by Western blotting. Figure 2B shows that FA causes a drastic decrease in the acetylation (Ac) of H3K9, H3K14, and H4K12 residues in the cytosolic fraction. Interestingly, the levels of these two modifications were increased in nuclear extract fractions but were slightly decreased in chromatin fractions following FA treatment (Figure 2B).

Effects of FA on the Deposition of Histone H3 into Chromatin

Acetylation of the N-terminal tails of H3 and H4 is critical for histone nuclear import and assembly into chromatin (Burgess and Zhang 2013). Thus, the reduction of cytosolic H3K9Ac, H3K14Ac and H4K12Ac by FA treatment may compromise the assembly of newly synthesized histones into chromatin. If this occurs, it should be expected that levels of nucleosomal histone H3 and H4 will be reduced after FA exposure. In fact, the amount of histone H3 in the chromatin fraction decreased by approximately

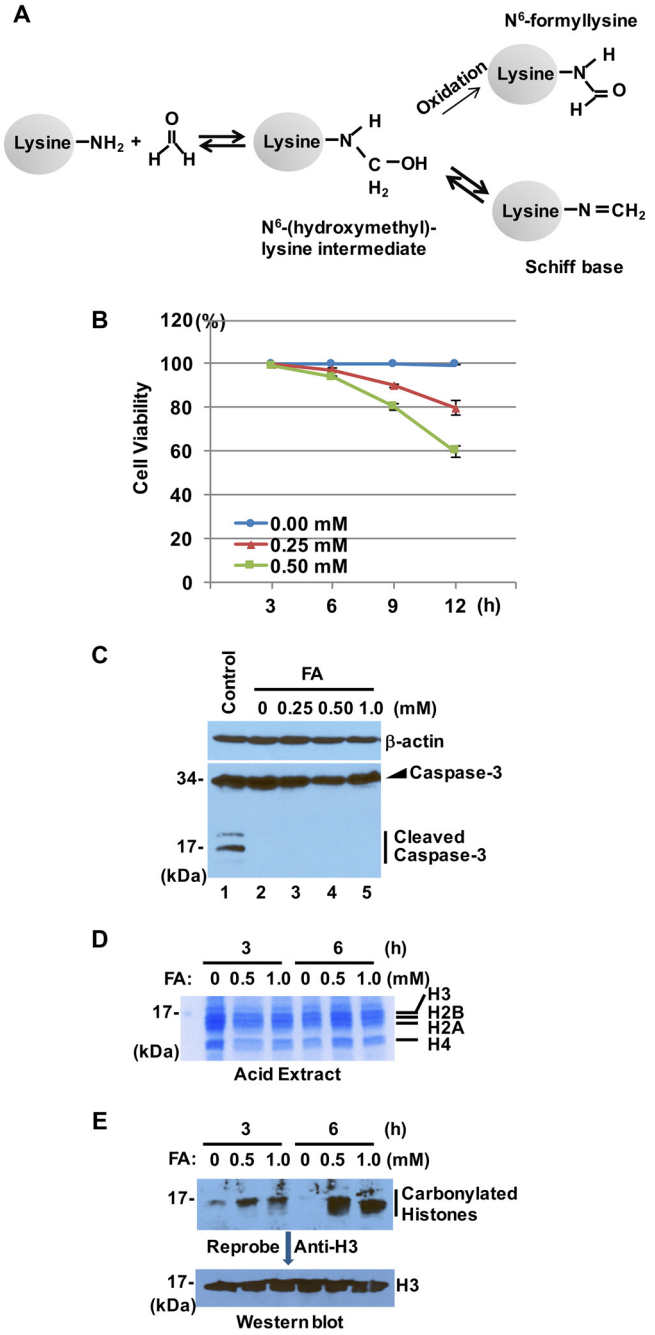

Figure 1. The formation of formaldehyde (FA)-histone adducts. (*A*) Typical reactions between FA and lysine residues of proteins with the formation of a Schiff base (primary FA-lysine adducts) and N^6-formyllysine, respectively. (*B*) Cytotoxicity of FA to BEAS-2B cells. Cells were exposed to FA, and cell viability was determined by trypan blue dye exclusion assays. Viability is presented as the percentage of live cells at each time point. Data represent the mean ± standard deviation (SD) of triplicate tests. (*C*) Whole-cell lysates were prepared from BEAS-2B cells treated with or without different concentrations of FA for 6 h and were subjected to Western blot analysis with antibodies against β-actin and caspase-3. No cleaved caspase-3 was observed in three independent experiments. (*D*) Coomassie blue staining of total histones isolated by acid extraction. (*E*) Representative immunoblot analysis of FA-histone adduct formation in cells ($n = 2$). Carbonylated proteins were detected with anti-dinitrophenyl (DNP) antibodies (upper panel). The same membrane was reprobed with anti-H3 antibodies (lower panel).

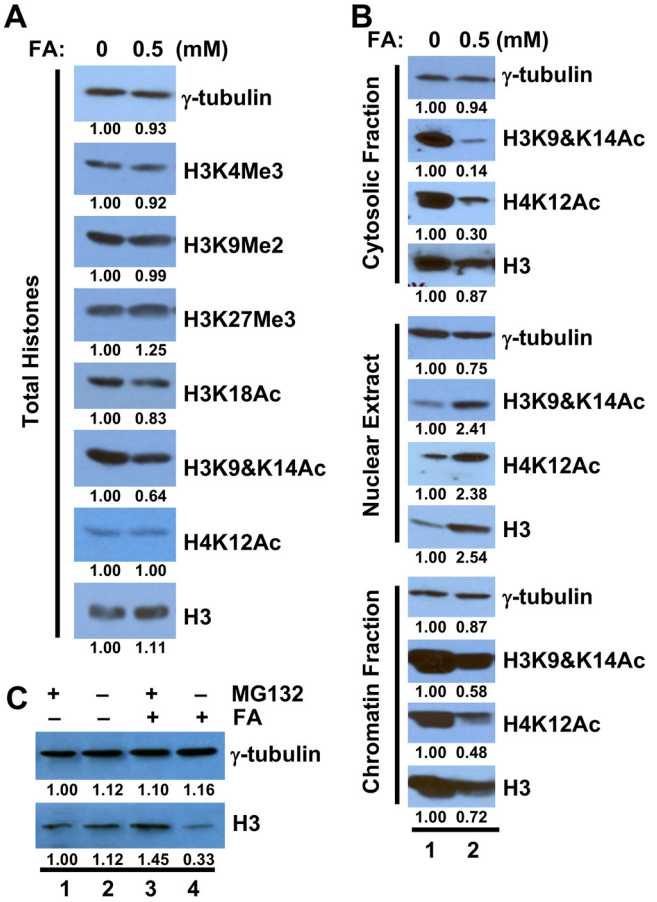

Figure 2. Effects of formaldehyde (FA) on acetylation of N-terminal tails of cytosolic histones. (*A*) BEAS-2B cells were exposed to FA for 6 h. Total histones were prepared by acid extraction and subjected to Western blot analysis. No marked decrease of histone modification was observed ($n = 2$). The band intensities were quantified using ImageJ (version 1.46r; National Institutes of Health) software. (*B*) Cytosolic fractions, nuclear extracts, and chromatin fractions were isolated from BEAS-2B cells treated with or without FA for 6 h and subjected to Western blot analysis. FA caused drastic decreases in cytosolic levels of H4K12Ac and H3K9&K14Ac ($n = 2$). (*C*) Cytosolic fractions were isolated from cells treated with or without FA (0.5 mM, 6 h) and the proteasome inhibitor MG132 (20 μM, 2 h) and then subjected to Western blot analysis. FA exposure increased cytosolic H3 in the presence of MG132 ($n = 2$).

20% (Figure 2B). The level of total H3 protein remained unchanged following FA exposure, making it unlikely that the observed reduction of H3 in the chromatin fraction is due to reduced expression of H3 (Figure 2A). Interestingly, FA increased the levels of total histone H3, H3K9Ac, H3K14Ac, and H4K12Ac in the nuclear extracts (Figure 2B). This finding implies that the delivery of histones to chromatin is blocked by FA exposure, resulting in the accumulation of FA-modified histones in the nuclear extract fraction. The levels of cytosolic H3 were also increased following FA exposure in the presence of the proteasome inhibitor MG132 (lanes 1 and 3; 2 and 4 in Figure 2C), suggesting that *a*) exposure to FA reduces histone nuclear import and *b*) aggregated FA-modified histones are degraded by the proteasome pathway. These critical observations reveal the activation of quality control mechanisms in histone homeostasis.

To further investigate the effects of FA exposure on chromatin assembly, we compared the levels of histones at a number of genomic loci before and after FA treatment. It was hypothesized that the inhibition of chromatin assembly would lead to a reduction of histone enrichment at specific genomic loci. ChIP assays were used to measure the amount of histone variant H3.3 at several genomic loci. The noncanonical histone variant H3.3 was used because it primarily localizes to active regions of the genome with high rates of histone turnover; thus, the impact of lack of histone supplies should be greatest in the H3.3 regions (Deal et al. 2010). The results of the ChIP assays clearly showed that the amount of H3.3 was significantly reduced at the majority of loci tested (Figure 3A). Taken together, we conclude that FA compromises chromatin assembly.

Effects of Physiologically Relevant Concentrations of FA on Acetylation of the N-Terminal Tails of Cytosolic Histones

We have used a relatively high dose of FA (0.5 mM) to demonstrate inhibition of histone modifications and chromatin assembly following FA exposure. Because epigenetic effects are considered to be nonlinear, it is important to test whether similar outcomes can be seen at a more physiologically relevant dose. It is reported that endogenous concentrations of FA in the blood are approximately 0.1 mM in rats, monkeys, and humans. Additionally, FA concentrations in the liver and nasal mucosa of the rat are 0.2 and 0.4 mM, respectively (Andersen et al. 2010; Casanova et al. 1988; Casanova-Schmitz et al. 1984; Heck and Casanova 2004; Heck et al. 1982, 1985). Based on these reports, it was determined that 100 μM FA is a physiologically relevant concentration. Relatively high levels of endogenous FA raised the question of whether the formation of FA–histone adducts could be a normal process. If so, environmental exposure to a physiologically relevant dose of FA may only slightly increase the burden of cellular toxicity. Exposure to FA could interfere with normal cellular processes because a major source of endogenous FA is from the demethylation of histones, RNA, and DNA within the nucleus (Walport et al. 2012), indicating that the level of endogenous FA in the cytoplasm might be relatively low. Thus, exposure to FA, which mainly targets cytoplasmic proteins, would have a significant impact on cytoplasmic processes even at physiological concentrations. Moreover, FA scavengers such as glutathione would be rapidly consumed by continuous exposure to the FA that we used in the experiments. To determine the effects of exogenous exposure to a physiologically relevant concentration of FA on cellular processes, we measured the levels of cytosolic H4K12Ac in several cell lines after they were exposed to 100 μM FA. The treatment significantly reduced the levels of cytosolic H4K12Ac in BEAS-2B cells, UTA6 cells (a human osteosarcoma cell line), and RPMI 2650 cells (a human nasal epithelial cell line) (Figure 3B); however, the time needed to induce the change varied from 24 h to 72 h among the different cell lines tested. The data suggest that continuous exposure of cells to physiological concentrations of FA significantly affects posttranslational modification of cytosolic histones at critical sites.

To determine whether nucleosome assembly is compromised after exposure to 100 μM FA, ChIP assays were performed to measure the amount of histone H3.3 in several genomic loci before and after FA exposure. H3.3 was depleted by FA treatment at the promoters of the genes that encode *EGR2, S100A10*, and *H3.3* (Figure 3C). This result indicates that nucleosome assembly in these sites is compromised following FA exposure at a physiologically relevant concentration.

Effects of FA on Chromatin Structure

Repression of histone expression interferes with chromatin assembly and enhances chromatin accessibility (Gossett and Lieb 2012). Chromatin accessibility could be affected by FA exposure through inhibition of chromatin assembly. MNase digestion

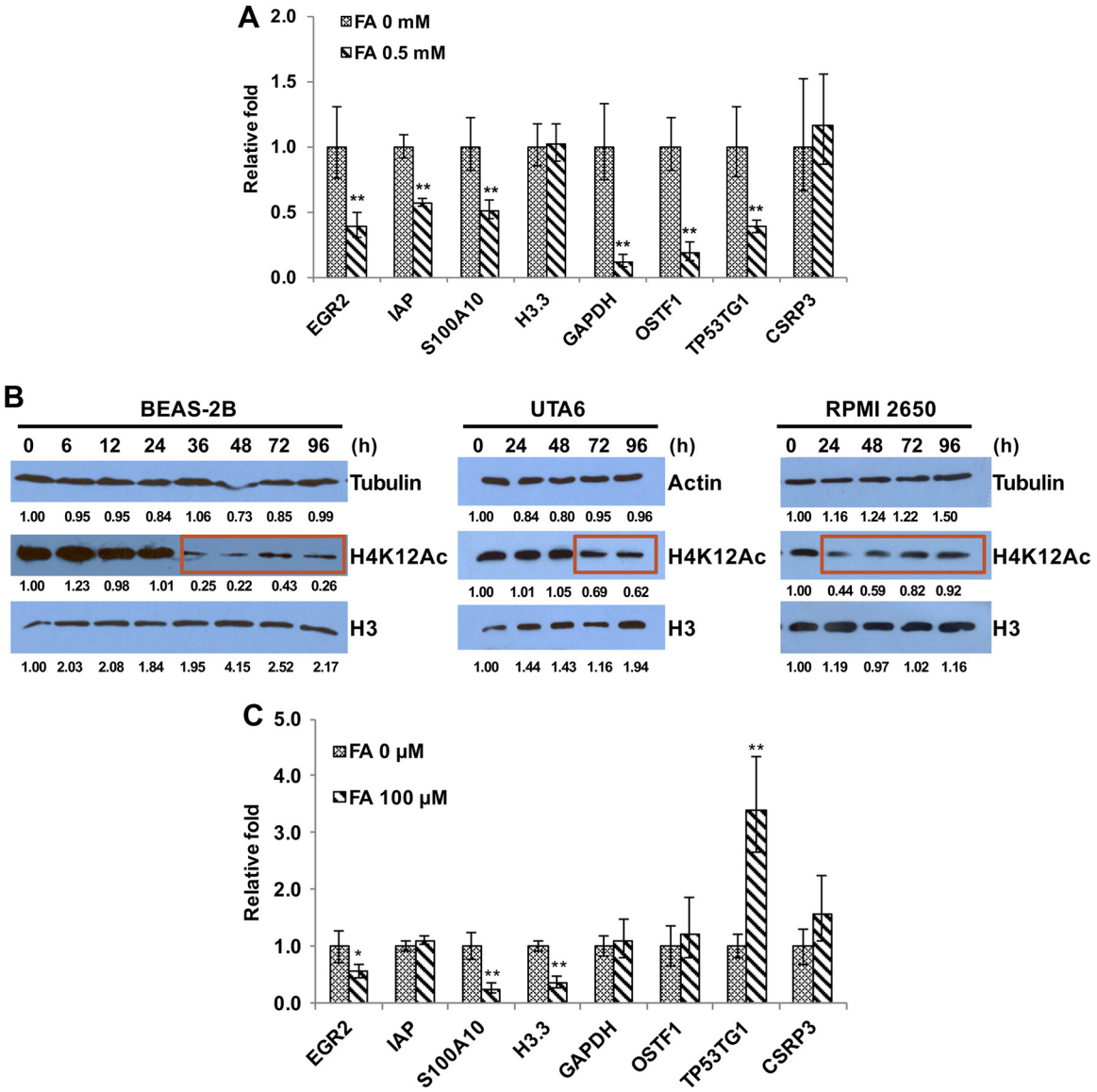

Figure 3. Effects of formaldehyde (FA) on H3.3-containing nucleosome assembly. (*A*) BEAS-2B cells with stable expression of FLAG-H3.3 were treated with or without FA for 6 h. Mono- and dinucleosomes were prepared and subjected to chromatin immunoprecipitation (ChIP) assays with FLAG antibodies to isolate FLAG-H3.3 nucleosomes. The data shown are the mean ± standard deviation (SD) from real-time quantitative polymerase chain reactions (qPCRs) performed in triplicate. $*p < 0.05$; $**p < 0.01$. The loci tested are mostly promoters except for GAPDH (gene body) and CSRP3 (gene end). Relative fold change was calculated after normalization to input and no antibody control. (*B*) Exposure to FA at physiologically relevant concentrations inhibits N-terminal tail acetylation of cytosolic histones. Cytosolic cell fractions were isolated from BEAS-2B cells, UTA6 cells, and RPMI 2650 cells treated with or without 100 μM FA and were subjected to Western blot analysis ($n = 2$). (*C*) Exposure of cells to physiologically relevant concentrations of FA compromises assembly of H3.3-containing nucleosomes. BEAS-2B cells with stable expression of FLAG-H3.3 were treated with or without FA for 48 h. Mono- and dinucleosomes were prepared and were subjected to ChIP assays to isolate FLAG-H3.3 nucleosomes. Data are the mean ± standard deviation (SD) from qPCRs performed in triplicate. $*p < 0.05$; $**p < 0.01$.

assays were used to investigate the influence of FA exposure on chromatin accessibility. Nuclei from BEAS-2B cells treated with or without FA were extracted and digested with MNase. Extracted DNA was then monitored for changes of protective monomer ladders by agarose gel electrophoresis. No changes were observed in cells treated with 0.25 mM FA (Figure 4A, lanes 1–6). However, exposure to 0.5 mM FA increased overall sensitivity to MNase. This effect was obvious when the nuclei were digested with 12×10^{-3} U/μL and 24×10^{-3} U/μL MNase, where the bands indicative of polynucleosomes (larger than 4-mers and 3-mers, respectively) were missing from FA-treated cells (arrowheads when comparing lanes 2 and 8; stars when comparing lanes 3 and 9). The general increase in chromatin accessibility with FA treatment suggests that nucleosome occupancy at genomic loci changed after FA exposure. MNase-qPCR was then utilized to determine the nucleosome occupancy at several genomic loci by measuring the ratio of the abundance of target DNA sequences in MNase-digested mononucleosomes isolated from FA-treated versus control cells (Jin and Felsenfeld 2006). As shown in Figure 4B, nucleosome occupancy decreased in the majority of sites we tested. Next, to investigate how MNase sensitivity is changed by exposure to physiological levels of FA, we performed MNase digestion assays after treating cells with 0.1 mM FA for 48 h. Figure 4C shows that when digested with 6×10^{-3} U/μL and 12×10^{-3} U/μL MNase, the intensities of the trinucleosome band (arrowheads when

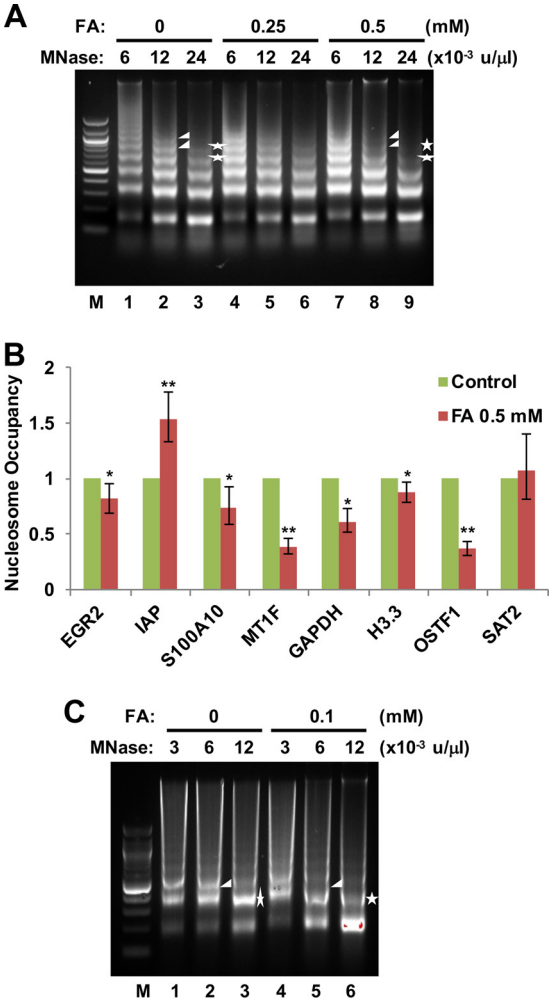

Figure 4. Effects of formaldehyde (FA) exposure on chromatin structure. (*A*) FA exposure increases chromatin accessibility. BEAS-2B cells were treated with or without FA for 6 h. Nuclei were isolated and digested with micrococcal nuclease (MNase). Digested DNA was extracted, electrophoretically separated on a 2% agarose gel, and visualized by ethidium bromide staining. Representative results from two independent experiments are shown. (*B*) Changes in nucleosome occupancy. MNase-digested monomeric DNA bands from untreated and FA-treated BEAS-2B cells were excised, and the DNA was extracted. The abundance of a sequence in protected nucleosomes was determined by real-time quantitative polymerase chain reactions (qPCRs) performed in triplicate. $*p < 0.05$; $**p < 0.01$. (*C*) Chromatin accessibility is increased with the exposure of cells to physiologically relevant doses of FA. BEAS-2B cells were treated with or without 0.1 mM FA for 48 h followed by MNase digest analysis as described in (*A*). Representative results from two independent experiments are shown.

comparing lanes 2 and 5) and the dinucleosome band (stars when comparing lanes 3 and 6), respectively, were greatly reduced following low-dose FA exposure (Figure 4C). Taken together, these data demonstrate that FA exposure can increase chromatin accessibility.

Characterization of Cancer-Related Genes Mediated by FA Exposure

Aberrant chromatin assembly can result in transcriptional defects. Thus, we hypothesized that the inhibition of chromatin assembly resulting from the formation of FA–histone adducts contributes to FA-mediated transcriptional dysregulation. RNA-seq was first used to characterize FA-inducible genes in BEAS-2B cells exposed to 100 μM FA for 48 h. DESeq (Anders and Huber 2010) was used to call differentially expressed genes in the RNA-seq data generated from two biological replicates (Feng et al. 2012) ($p < 0.05$). A total of 654 genes were identified as FA-responsive genes (see Table S1). Figure 5A shows an RNA-Seq heatmap for differentially expressed genes. Ingenuity Pathway Analysis (IPA) was then used to annotate the data set and to analyze the data in the context of biological processes, pathways, and networks. Top diseases and biological functions related to this data set were dermatological diseases, cancer, inflammatory response, tumor morphology, and neurological disease (Figure 5B).

It is important to note that of 654 FA-responsive genes, 361 were identified as cancer-related. Signaling pathway analysis showed that these genes were involved in several pathways, including p53 signaling, HER-2 signaling, and Wnt/beta-catenin signaling (Figure 5C). Interestingly, leukemia signaling was present in these cancer pathways, providing a potential mode of action for FA-induced leukemia. To validate the RNA-seq results, eight up-regulated and eight down-regulated genes were selected for qPCR analysis. The selected genes included well-known oncogenes such as *FOS* and *JUN* and tumor suppressors such as *CDKN1A* and *SERPINB5* from the top and bottom 60 FA-responsive genes (Tables 3 and 4). All 16 selected genes are associated with head/neck neoplasia, hematological neoplasia, or both (Tables 3 and 4). The similar tendency of differential expression with FA treatment of all of the selected genes was observed with RT-qPCR as shown with RNA-seq (Figure 6A, B). The functional and RT-qPCR analyses demonstrate that the RNA-seq data were reliable and confirm that the selected 16 cancer-related genes were dysregulated following FA exposure.

Effects of Chromatin Assembly Inhibition on Expression of FA-Responsive Cancer-Related Genes

To delineate the contribution of defective chromatin assembly in FA-mediated dysregulation of gene expression, we examined how the expression of the selected 16 cancer-related genes was influenced by knockdown of the histone variant H3.3. Because knockdown of H3.3 disrupts chromatin assembly, the overlap between transcriptional patterns generated by H3.3 knockdown and FA exposure may represent the genes regulated by FA-induced aberrant chromatin assembly. Expression of canonical histones H3.1 and H3.2 peaks during S phase, and their assembly is replication-dependent. By contrast, H3 variant H3.3 is expressed throughout the cell cycle, and its assembly is not dependent on DNA replication (Szenker et al. 2011). Moreover, H3.3 is mainly localized at active regions with high rates of histone turnover (Deal et al. 2010). Thus, the assembly of H3.3 should be affected first and to the greatest extent by a lack of histone supplies. Knockdown of histone variant H3.3 was carried out using two distinct siRNAs. The knockdown efficiencies of H3.3 mRNA were approximately 74% and 60% in cells transfected with H3.3 siRNA 1 and H3.3 siRNA 2, respectively, compared with control siRNA (Figure 6c). Western blot analysis showed that the protein levels of FLAG-H3.3 and most likely endogenous H3.3 were reduced by transfection of both siRNAs for H3.3 (Figure 6D). Six of the eight genes that were highly up-regulated by FA exposure (including *FOS, JUN*, and *JUNB*) and three of the eight highly down-regulated genes (including *CDKN1A* and *SERPINB5*) were also abnormally expressed as a result of H3.3 knockdown (Figure 6E, F; see also Figure S2). These results suggest that aberrant chromatin assembly dysregulates expression of FA-responsive cancer-related genes and may play an important role in FA-induced carcinogenesis.

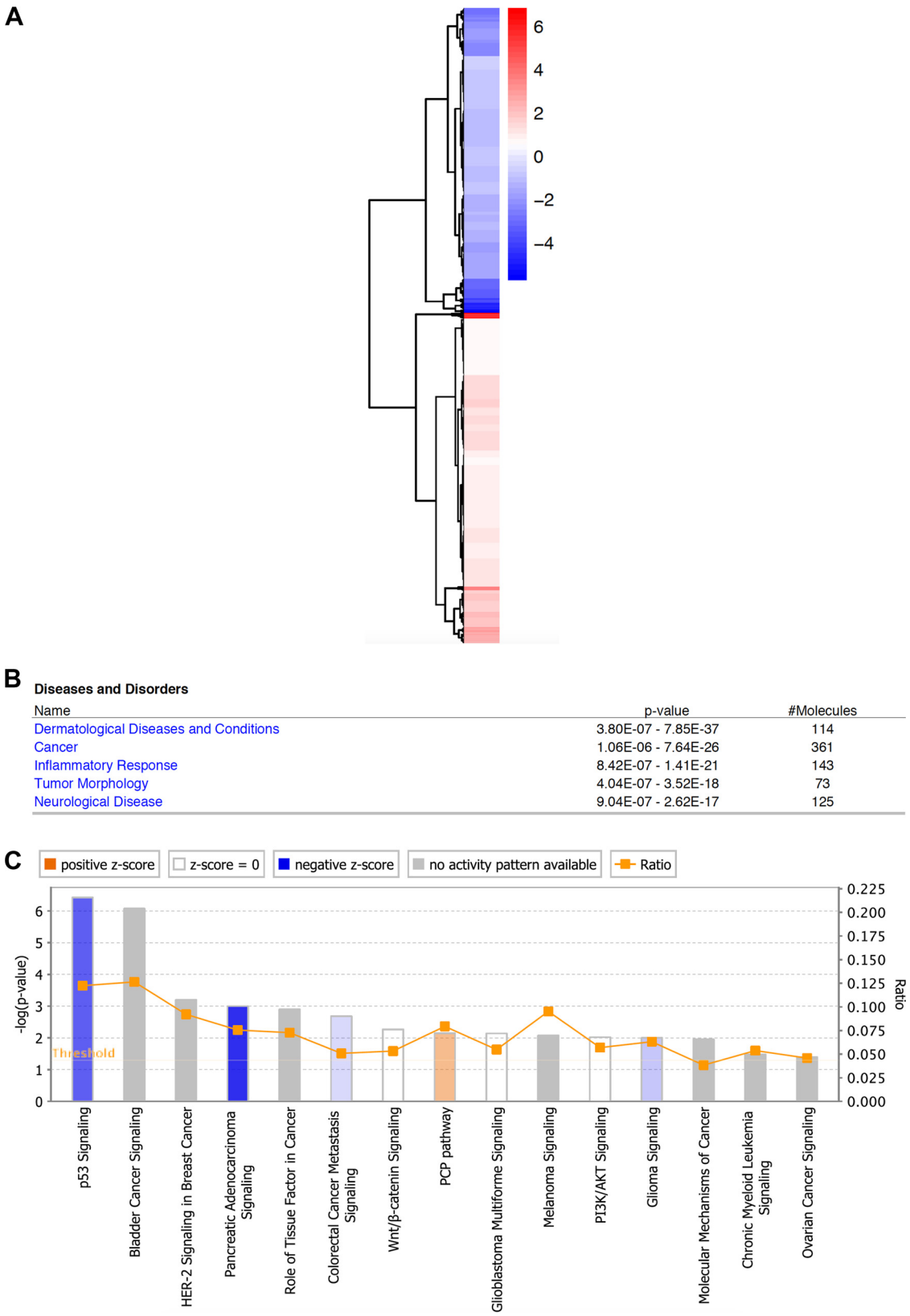

Figure 5. Ingenuity Pathway Analysis (IPA) of formaldehyde (FA)-induced genes. (*A*) RNA sequencing (RNA-Seq) heatmap for differentially expressed genes. Color represents the $\log_2$-fold changes between FA-treated and untreated cells. (*B*) The top five diseases and biological functions related to 654 FA-responsive genes are shown. (*C*) Signaling pathways, including chronic myeloid leukemia signaling, are associated with FA-responsive cancer-related genes.

Table 3. Up-regulated genes selected for validation and further analysis.

Gene ID	Fold	p-Value	Head/neck cancer	Head/neck neoplasia	Hematological neoplasia
HES1	53.04726729	3.26×10^{-34}		X	X
FOS	50.99508222	1.38×10^{-45}		X	
EGR1	18.0602504	4.88×10^{-31}	X	X	X
DUSP1	5.2543302	5.69×10^{-15}	X	X	
LAMA4	3.830065786	0.002178393	X	X	
JUN	3.782087529	3.75×10^{-10}			X
JUNB	3.668838129	3.07×10^{-9}			X
CDH1	3.499623281	0.014377408	X	X	

Table 4. Down-regulated genes selected for validation and further analysis.

Gene ID	Fold	p-Value	Head/neck cancer	Head/neck neoplasia	Hematological neoplasia
CDKN1A	0.20440373	7.31×10^{-9}	X	X	X
MMP3	0.198641845	0.0015294		X	
CSF2	0.197596408	1.23×10^{-9}		X	X
CCND1	0.112553466	9.18×10^{-19}	X	X	X
HMGA2	0.105126004	1.59×10^{-12}		X	X
SERPINB5	0.099067363	0.000024			X
MYEOV	0.020476397	0.0000394	X	X	
MMP1	0.01893875	2.88×10^{-23}	X	X	

Effects of H3.3 Knockdown on Anchorage-Independent Growth of BEAS-2B Cells

A hallmark of carcinogenesis *in vitro* is the cell's acquired ability of anchorage-independent growth in soft agar. To examine whether cells gained this property following FA exposure at physiologically relevant concentrations, BEAS-2B cells were treated with 100 μM FA for 24 h or 48 h, plated in soft agar, and cultured for 5 wk. Exposure to FA greatly enhanced colony formation when cells were treated for 48 h but not for 24 h (Figure 7A), indicating that cells exposed to physiologically relevant doses of FA can acquire this hallmark chartacteristic of cell transformation. Interestingly, the level of cytosolic H4K12Ac also decreased only when cells were exposed to 100 μM FA for 36 h or longer but not for 24 h (Figure 3B). In conjunction with previous observations, reduction of acetylation of N-terminal tails of cytosolic histone(s) and the subsequent inhibition of chromatin assembly might play a role in FA-induced cell transformation.

To examine whether defective chromatin assembly may have contributed to FA-induced anchorage-independent cell growth, we performed soft agar assays. siRNA knockdown of H3.3 was utilized to mimic partial inhibition of chromatin assembly. BEAS-2B cells were transiently transfected with control siRNA or H3.3 siRNA in the presence or absence of 100 μM FA for 48 h. Knockdown efficiency was confirmed by RT-qPCR and Western blot analysis (Figure 6C, D). Unexpectedly, the control siRNA induced colony formation of BEAS-2B cells in soft agar (Figure 7B). It is possible that the control siRNA may have randomly targeted some genes related to colony formation of cells in soft agar. Notably, colony formation in soft agar was significantly enhanced by knockdown of H3.3 compared with the control siRNA (Figure 7B; see also Figure S3). Additionally, reduction of H3.3 facilitated FA-mediated anchorage-independent growth of BEAS-2B cells (Figure 7B; see also Figure S3).

Discussion

In this study, we demonstrated a reduction in lysine acetylation of the cytosolic histones H3 and H4 and inhibition of chromatin assembly following FA exposure. Inhibition of chromatin assembly altered the expression of a number of cancer-related genes and networks. Exposure to FA also facilitated anchorage-independent growth of BEAS-2B cells. The ability of FA to react with certain lysine residues on newly synthesized histones and to subsequently compromise chromatin assembly represents a potentially novel mechanism for the toxic and carcinogenic effects of FA.

FA reacts with lysine residues of proteins to form a Schiff base or N^6-formyllysine. Both Schiff bases and N^6-formyllysine are resistant to physiological modifications, such as acetylation. Although acetylated lysine is chemically unequivocal from a Schiff base, formylated lysine and acetylated lysine are quite similar to each other. However, there are several reasons why lysine formylation might have significant biological consequences. If formylated and acetylated lysines share similar biological responses, formylated lysines should be removed as efficiently as acetylated lysines by lysine deacetylases, which remove acetyllysine from histones. Previous work has revealed that lysine formylation is not affected by treatment of cells with histone deacetylases (Edrissi et al. 2013a). Moreover, although a histone deacetylase completely removed the acetyl modification from peptides *in vitro*, only $\sim 10\%$ of formyllysine was removed enzymatically (Edrissi et al. 2013a). This observation suggests that formyllysine and acetyllysine have very different biochemical reactivities. Unlike lysine acetylation, which is transient, formyllysine is considered to persist throughout the lifetime of individual histone proteins. For instance, the H4K5Ac and H4K12Ac are removed 20–60 min after deposition (Jackson et al. 1976; Taddei et al. 1999). These marks are also required for the maturation of chromatin, as demonstrated for pericentric heterochromatin (Annunziato and Seale 1983; Ekwall et al. 1997; Taddei et al. 2001). The persistence of formylated lysines could disrupt the chromatin landscape. For-myllysine is stable and may also inhibit lysine methylation (Edrissi et al. 2013a; Jiang et al. 2007); methylated lysine has chemical properties distinct from those of acetylated lysine (Rice and Allis 2001). Thus, both lysine formylation and Schiff base formation should interfere with signaling processes associated with acetylation.

Cell fractionation to isolate cytosolic, nuclear, and chromatin fractions (Chen et al. 2013) demonstrated that FA mainly downregulated acetylation of cytosolic histones H3 and H4. It should be noted that this change was not an expected outcome (Figure 2B). Histone PTMs have been classically analyzed using total histones as substrates. However, this approach cannot distinguish changes in subcellular distribution, and it might not be sensitive

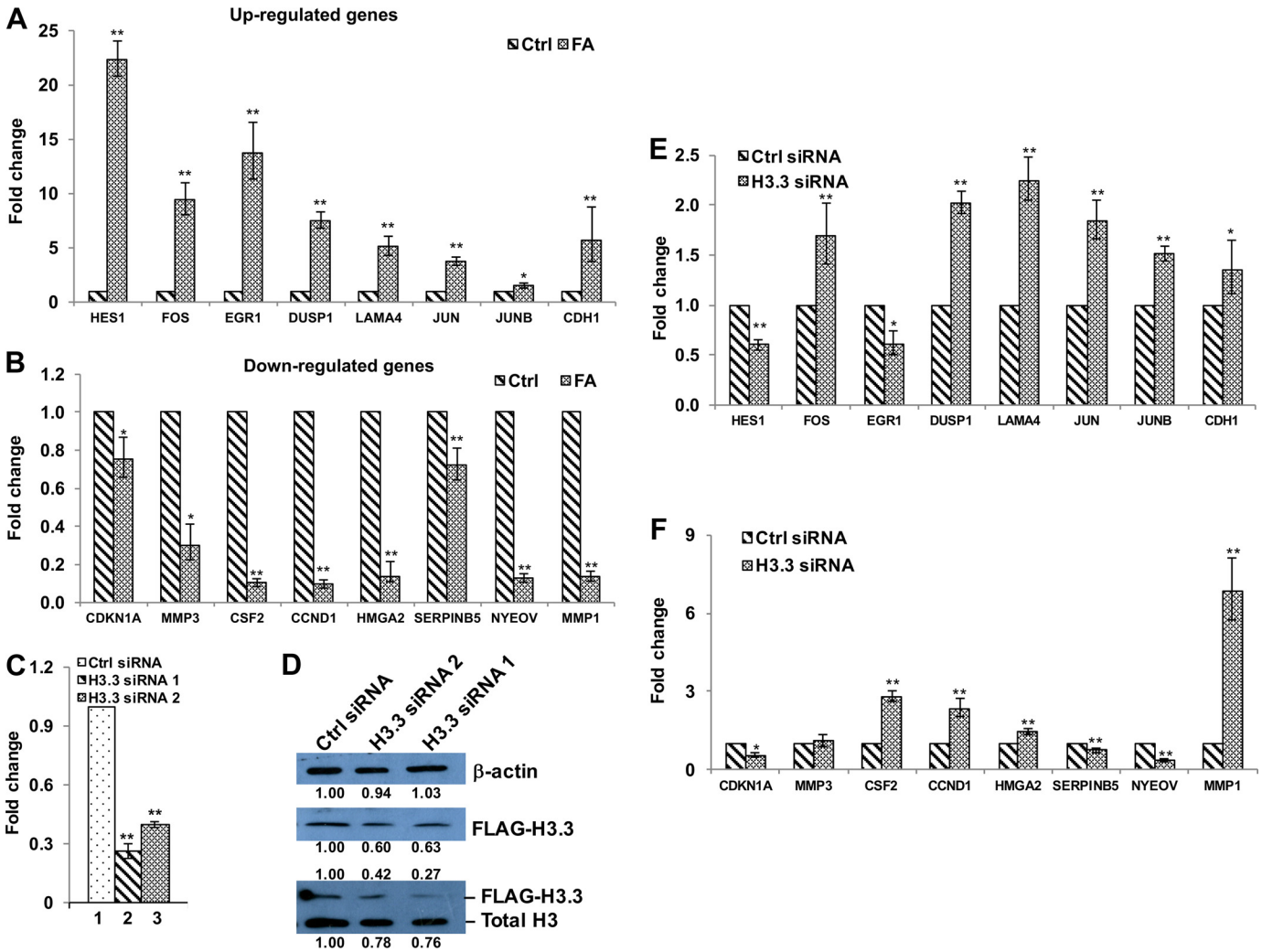

Figure 6. Effects of H3.3 knockdown on the expression of formaldehyde (FA)-responsive genes. (*A*, *B*) Real-time polymerase chain reaction (PCR) validation of RNA sequencing (RNA-seq) results. Eight up-regulated (*A*) and eight down-regulated (*B*) cancer-related genes following exposure to FA (100 μM for 48 h) in BEAS-2B cells were selected from RNA-seq results. mRNA levels of these genes were analyzed by reverse transcriptase quantitative real-time PCR (RT-qPCR). Differential expression of these genes was in accord with the RNA-seq results. Data are the mean ± standard deviation (SD). ($n = 3$). $*p < 0.05$; $**p < 0.01$. (*C*) RT-qPCR analysis of H3.3 mRNA levels in BEAS-2B cells after 48-h transfection with control (Ctrl) short interfering RNA (siRNA), H3.3 siRNA 1, or H3.3 siRNA 2. (*D*) Western blot analysis of ectopic H3.3 protein levels in BEAS-2B cells after 48-h transfection with control (Ctrl) siRNA or with two distinct siRNAs for H3.3 (H3.3 siRNA 1 and H3.3 siRNA 2). Antibodies against β-actin (top), FLAG (middle), or H3 (bottom) were used. (*E*, *F*) RT-qPCR measurements of transcripts of the indicated FA-responsive cancer-related genes in H3.3 knockdown and control cells. The data shown are the mean ± standard deviation (SD). ($n = 3$). $*p < 0.05$; $**p < 0.01$.

enough to detect changes in cytosolic histone modifications even when they are dramatic because cytosolic histones represent only a small percentage of total histones (Loyola et al. 2006). Thus, the change might not have been observed if total histones had been analyzed without prior cell fractionation. FA compromised chromatin assembly, indicated by the reduction of histone proteins in the chromatin fraction and the depletion of histone variant H3.3 at genomic loci following FA exposure. In addition, the amount of cytosolic histone H3 was increased with FA treatment in the presence of MG132, suggestive of accumulation of histone proteins in cytoplasm following FA treatment. Interestingly, a dramatic increase in the levels of histones H3 and H4 marked with H4K12Ac in nuclear fractions after FA exposure was also observed. Histone nuclear import and assembly into chromatin is a dynamic process. Histone deposition to chromatin requires both histone H3 and H4 tails, whereas histone nuclear import only requires H4 tails (Ejlassi-Lassallette et al. 2011), suggesting that histone deposition to chromatin could be compromised to a greater extent than that of histone nuclear import. For example, an H3/H4 complex with abnormal H3 tail acetylation could be imported into the nucleus but be blocked in the nuclear fraction, resulting in an increase in the acetylated histone (in this case, acetylated H4) level in the nuclear fraction. This may explain our observation of more histones in the nuclear fraction of FA-treated cells than in untreated cells. These results support the idea that FA exposure compromises histone nuclear import and assembly into chromatin.

Aberrant chromatin assembly could contribute to the development of cancer because it can induce defects in DNA repair, replication, and transcription to cause genomic instability (Ransom et al. 2010). If it is not repaired, DNA damage can accumulate, leading to mutations and cancer. Defects in chromatin assembly, caused by a loss of either histones or histone chaperones, interfere with DNA repair processes. For example, reduction of H2A.X levels influences γ-H2A.X densities along damage sites, thereby affecting repair processes (Savic et al. 2009). Histone H2A.Z

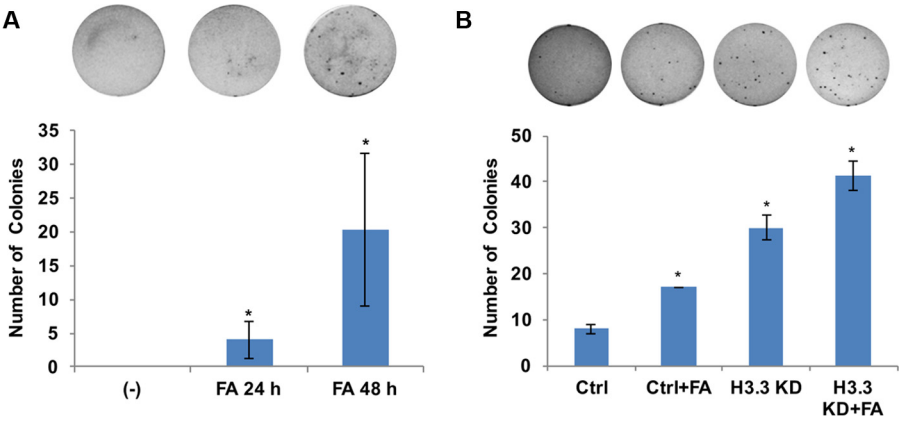

Figure 7. Effects of H3.3 knockdown on anchorage-independent growth of BEAS-2B cells. (*A*) Formaldehyde (FA) facilitates colony formation of BEAS-2B cells on soft agar. After FA treatment (100 μM), the cells were plated in 0.35% soft agar and cultured for 5 wk. (*B*) BEAS-2B cells were transiently transfected with control siRNA (Ctrl) or with H3.3 siRNA 1 (H3.3 KD) in the presence or absence of 100 μM FA for 48 h. The cells were then plated in 0.35% soft agar and cultured for 4 wk. The data shown are the mean ± standard deviation (SD) from experiments performed in triplicate. $^*p < 0.01$.

promotes DNA end resection, and knockout of H2A.Z increases sensitivity to DNA damage (Soria et al. 2012). Histone chaperones CAF-1 and FACT are involved in deposition of new H3.1-H4 and H2A-H2B, respectively, to restore chromatin after DNA repair, which is important for turning off the DNA damage checkpoint (Dinant et al. 2013; Soria et al. 2012). Nucleosome deposition by CAF-1 following mismatch removal prevented the nascent DNA strand from excessive degradation by the mismatch repair (MMR) machinery (Kadyrova et al. 2011; Schöpf et al. 2012). In addition, the impairment of DNA replication by abnormal chromatin assembly during S phase is a direct cause of genetic instability and is associated with early tumor development. For instance, depletion of CAF-1 profoundly decreased the assembly of newly replicated DNA into chromatin and stalled DNA replication, caused DNA double-strand breaks, and activated the S phase checkpoint (Hoek and Stillman 2003; Ye and Adams 2003). Moreover, Asf1 depletion resulted in chromosomal aberrations and micronuclei formation, and repression of histone H4 impaired chromosomal segregation and increased genomic instability (Prado and Aguilera 2005). Depletion of H2B also rendered cells incapable of chromosomal segregation (Saunders et al. 1990). Furthermore, aberrant chromatin assembly dysregulates transcription of cancer-related genes (Gossett and Lieb 2012). Therefore, FA-induced inhibition of chromatin assembly could hypothetically be a significant contributor to FA-induced cancer. In line with this hypothesis, partial inhibition of chromatin assembly by knocking down H3.3 did enhance colony formation in soft agar and facilitate FA-mediated anchorage-independent growth of BEAS-2B cells.

Most research on FA carcinogenesis has focused on DNA damage and on the resulting mutagenesis induced by the formation of DNA adducts and DNA-protein cross-links (DPCs) (Swenberg et al. 2013). However, it was expected that mechanisms other than genetic damage may play a role in FA-induced carcinogenesis because exogenous FA caused only a modest increase in DNA adducts above the levels caused by endogenous FA (Lu et al. 2010; Lu et al. 2011; Moeller et al. 2011; Swenberg et al. 2011). We now provide evidence that inhibition of chromatin assembly due to reduced acetylation of N-terminal tails of cytosolic histones may contribute to FA-mediated carcinogenicity. Although epidemiology studies have linked FA exposure to leukemia (Goldstein 2011; Zhang et al. 2010a), the mode of action was not clear. In particular, DNA adducts were not detectable in the bone marrow of animals exposed to FA. Using RNA-seq, we have identified a number of tumor suppressor genes and oncogenes altered by FA exposure. Among them, at least *HES1, EGR1, JUN, JUNB, CDKN1A, CSF2, CCND1, HMGA2*, and *SERPINB5* have been associated with hematological neoplasia (see Tables 3 and 4). Notably, *JUN, JUNB, CDKN1A*, and *SERPINB5* were also dysregulated by H3.3 knockdown, suggesting that inhibition of chromatin assembly might play a role in the development of leukemia associated with FA exposure.

Chromatin assembly can be regulated by histone modifications and by other factors such as histone chaperone proteins (Burgess and Zhang 2013). Although it is clear that FA–histone lysine adduct formation prevents the sites from being "physiologically" acetylated by HAT, the possibility that the expression or enzymatic activity of histone-modifying enzymes is also influenced by FA exposure cannot be ruled out. These aberrant reactions may lead to protein degradation or to altered protein function (Jacobs and Marnett 2010), implying that FA may change histone modifications by reacting with histone-modifying enzyme(s) such as HAT1, which is specific for H4K5 and H4K12 acetylation. It is also possible that FA forms adducts with amino acid residues of histone chaperones, such as CAF-1, HIRA and ASF1, as well as with histone translocator proteins, such as Importin 4. This protein interaction could influence their expression or interfere with their activities. To clarify mechanisms involved in FA-induced changes in histone modification and chromatin assembly, it is important to determine if the expression levels and activities of HATs, histone chaperones, and translocation factors are changed following FA exposure.

FA forms adducts with histone proteins, which have molecular weights of approximately 17 kDa (Figure 1). It is possible that other proteins of similar size also form adducts with FA and play a role in FA-related carcinogenesis. Using mass spectrometry, we will not only determine the sites of amino acid residues on histone proteins that interact with FA in cells and *in vivo* but also track the full spectrum of modified proteins in the future. Another limitation of this study is that we used immortalized human bronchial epithelial cells in most of our experiments. It is important to confirm whether similar responses to FA exposure can be observed with normal human nasal epithelial cells.

Conclusion

In conclusion, FA formed adducts with histone proteins and specifically inhibited covalent modifications of cytosolic histones H3 and H4, leading to aberrant chromatin assembly in BEAS-2B

cells. Defective chromatin assembly resulted in changes in the expression of a number of cancer-related genes and facilitated anchorage-independent growth of BEAS-2B cells. Inhibition of chromatin assembly appears to play an important role in FA-induced carcinogenesis. Because other electrophilic carcinogens could produce similar effects, we propose that blocking chromatin assembly represents a novel mechanism by which certain chemical carcinogens lead to the development of cancer.

References

Ahmad K, Henikoff S. 2002. The histone variant H3.3 marks active chromatin by replication-independent nucleosome assembly. Mol Cell 9(6):1191–1200, PMID: 12086617, https://doi.org/10.1016/S1097-2765(02)00542-7.

Anders S, Huber W. 2010. Differential expression analysis for sequence count data. Genome Biol 11(10):R106, PMID: 20979621, https://doi.org/10.1186/gb-2010-11-10-r106.

Andersen ME, Clewell HJ 3rd, Bermudez E, Dodd DE, Willson GA, Campbell JL, et al. 2010. Formaldehyde: Integrating dosimetry, cytotoxicity, and genomics to understand dose-dependent transitions for an endogenous compound. Toxicol Sci 118(2):716–731, PMID: 20884683, https://doi.org/10.1093/toxsci/kfq303.

Annunziato AT, Seale RL. 1983. Histone deacetylation is required for the maturation of newly replicated chromatin. J Biol Chem 258(20):12675–12684, PMID: 6226660.

Burgess RJ, Zhang Z. 2013. Histone chaperones in nucleosome assembly and human disease. Nat Struct Mol Biol 20(1):14–22, PMID: 23288364, https://doi.org/10.1038/nsmb.2461.

Burgess RJ, Zhou H, Han J, Zhang Z. 2010. A role for Gcn5 in replication-coupled nucleosome assembly. Mol Cell 37(4):469–480, PMID: 20188666, https://doi.org/10.1016/j.molcel.2010.01.020.

Casanova M, Heck HD, Everitt JI, Harrington WW Jr, Popp JA. 1988. Formaldehyde concentrations in the blood of rhesus monkeys after inhalation exposure. Food Chem Toxicol 26(8):715–716, PMID: 3198038, https://doi.org/10.1016/0278-6915(88)90071-3.

Casanova M, Morgan KT, Stemhagen WH, Everitt JI, Popp JA, Heck HD. 1991. Covalent binding of inhaled formaldehyde to DNA in the respiratory tract of rhesus monkeys: Pharmacokinetics, rat-to-monkey interspecies scaling, and extrapolation to man. Toxicol Sci 17(2):409–428, PMID: 1765228, https://doi.org/10.1093/toxsci/17.2.409.

Casanova-Schmitz M, David RM, Heck HD. 1984. Oxidation of formaldehyde and acetaldehyde by NAD+-dependent dehydrogenases in rat nasal mucosal homogenates. Biochem Pharmacol 33(7):1137–1142, PMID: 6477684, https://doi.org/10.1016/0006-2952(84)90526-4.

Chen D, Fang L, Li H, Tang MS, Jin C. 2013. Cigarette smoke component acrolein modulates chromatin assembly by inhibiting histone acetylation. J Biol Chem 288(30):21678–21687, PMID: 23770671, https://doi.org/10.1074/jbc.M113.476630.

Deal RB, Henikoff JG, Henikoff S. 2010. Genome-wide kinetics of nucleosome turnover determined by metabolic labeling of histones. Science 328(5982):1161–1164, PMID: 20508129, https://doi.org/10.1126/science.1186777.

Dinant C, Ampatziadis-Michailidis G, Lans H, Tresini M, Lagarou A, Grosbart M, et al. 2013. Enhanced chromatin dynamics by fact promotes transcriptional restart after uv-induced DNA damage. Mol Cell 51(4):469–479, PMID: 23973375, https://doi.org/10.1016/j.molcel.2013.08.007.

Dobin A, Davis CA, Schlesinger F, Drenkow J, Zaleski C, Jha S, et al. 2013. STAR: Ultrafast universal RNA-seq aligner. Bioinformatics 29(1):15–21, PMID: 23104886, https://doi.org/10.1093/bioinformatics/bts635.

Edrissi B, Taghizadeh K, Dedon PC. 2013a. Quantitative analysis of histone modifications: Formaldehyde is a source of pathological N^6-formyllysine that is refractory to histone deacetylases. PLoS Genet 9(2):e1003328, PMID: 23468656, https://doi.org/10.1371/journal.pgen.1003328.

Edrissi B, Taghizadeh K, Moeller BC, Kracko D, Doyle-Eisele M, Swenberg JA, et al. 2013b. Dosimetry of N^6-formyllysine adducts following [$^{13}C^2H_2$]-formaldehyde exposures in rats. Chem Res Toxicol 26(10):1421–1423, https://doi.org/10.1021/tx400320u.

Ejlassi-Lassallette A, Mocquard E, Arnaud MC, Thiriet C. 2011. H4 replication-dependent diacetylation and Hat1 promote S-phase chromatin assembly in vivo. Mol Biol Cell 22(2):245–255, PMID: 21118997, https://doi.org/10.1091/mbc.E10-07-0633.

Ejlassi-Lassallette A, Thiriet C. 2012. Replication-coupled chromatin assembly of newly synthesized histones: Distinct functions for the histone tail domains. Biochem Cell Biol 90(1):14–21, PMID: 22023434, https://doi.org/10.1139/o11-044.

Ekwall K, Olsson T, Turner BM, Cranston G, Allshire RC. 1997. Transient inhibition of histone deacetylation alters the structural and functional imprint at fission yeast centromeres. Cell 91(7):1021–1032, PMID: 9428524, https://doi.org/10.1016/S0092-8674(00)80492-4.

Feng J, Meyer CA, Wang Q, Liu JS, Shirley Liu X, Zhang Y. 2012. GFOLD: A generalized fold change for ranking differentially expressed genes from RNA-seq data. Bioinformatics 28(21):2782–2788, PMID: 22923299, https://doi.org/10.1093/bioinformatics/bts515.

Galligan JJ, Marnett LJ. 2017. Histone adduction and its functional impact on epigenetics. Chem Res Toxicol 30:376–387, PMID: 27930886, https://doi.org/10.1021/acs.chemrestox.6b00379.

Goldstein BD. 2011. Hematological and toxicological evaluation of formaldehyde as a potential cause of human leukemia. Hum Exp Toxicol 30(1):725–735, PMID: 20729258, https://doi.org/10.1177/0960327110381682.

Gossett AJ, Lieb JD. 2012. *In vivo* effects of histone H3 depletion on nucleosome occupancy and position in *Saccharomyces cerevisiae*. PLoS Genet 8(6):e1002771, PMID: 22737086, https://doi.org/10.1371/journal.pgen.1002771.

Hauptmann M, Lubin JH, Stewart PA, Hayes RB, Blair A. 2004. Mortality from solid cancers among workers in formaldehyde industries. Am J Epidemiol 159(12):1117–1130, PMID: 15191929, https://doi.org/10.1093/aje/kwh174.

Heck H, Casanova M. 2004. The implausibility of leukemia induction by formaldehyde: A critical review of the biological evidence on distant-site toxicity. Regul Toxicol Pharmacol 40(2):92–106, PMID: 15450713, https://doi.org/10.1016/j.yrtph.2004.05.001.

Heck HD, Casanova-Schmitz M, Dodd PB, Schachter EN, Witek TJ, Tosun T. 1985. Formaldehyde (CH_2O) concentrations in the blood of humans and Fischer-344 rats exposed to CH_2O under controlled conditions. Am Ind Hyg Assoc J 46(1):1–3, PMID: 4025145, https://doi.org/10.1080/15298668591394275.

Heck HD, White EL, Casanova-Schmitz M. 1982. Determination of formaldehyde in biological tissues by gas chromatography/mass spectrometry. Biomed Mass Spectrom 9(8):347–353, PMID: 7126766, https://doi.org/10.1002/bms.1200090808.

Hoek M, Stillman B. 2003. Chromatin assembly factor 1 is essential and couples chromatin assembly to DNA replication *in vivo*. Proc Natl Acad Sci USA 100(21):12183–12188, PMID: 14519857, https://doi.org/10.1073/pnas.1635158100.

IARC (International Agency for Research on Cancer). 2012. Formaldehyde. In: A Review of Human Carcinogens. Part F: Chemical Agents and Related Occupations. Monogr Eval Carcinog Risk Hum 100:401–435, monographs. iarc.fr/ENG/Monographs/vol100F/mono100F.pdf [accessed 10 June 2013].

Jackson V, Shires A, Tanphaichitr N, Chalkley R. 1976. Modifications to histones immediately after synthesis. J Mol Biol 104(2):471–483, PMID: 950668.

Jacobs AT, Marnett LJ. 2010. Systems analysis of protein modification and cellular responses induced by electrophile stress. Acc Chem Res 43(5):673–683, PMID: 20218676, https://doi.org/10.1021/ar900286y.

Jiang T, Zhou X, Taghizadeh K, Dong M, Dedon PC. 2007. N-Formylation of lysine in histone proteins as a secondary modification arising from oxidative DNA damage. Proc Natl Acad Sci USA 104(1):60–65, PMID: 17190813, https://doi.org/10.1073/pnas.0606775103.

Jin C, Felsenfeld G. 2006. Distribution of histone H3.3 in hematopoietic cell lineages. Proc Natl Acad Sci USA 103(3):574–579, PMID: 16407103, https://doi.org/10.1073/pnas.0509974103.

Jin C, Felsenfeld G. 2007. Nucleosome stability mediated by histone variants H3.3 and H2A.Z. Genes Dev 21(12):1519–1529, PMID: 17575053, https://doi.org/10.1101/gad.1547707.

Kadyrova LY, Blanko ER, Kadyrov FA. 2011. CAF-I-dependent control of degradation of the discontinuous strands during mismatch repair. Proc Natl Acad Sci USA 108(7):2753–2758, PMID: 21282622, https://doi.org/10.1073/pnas.1015914108.

Kerns WD, Pavkov KL, Donofrio DJ, Gralla EJ, Swenberg JA. 1983. Carcinogenicity of formaldehyde in rats and mice after long-term inhalation exposure. Cancer Res 43(9):4382–4392, PMID: 6871871.

Kouzarides T. 2007. Chromatin modifications and their function. Cell 128(4):693–705, PMID: 17320507, https://doi.org/10.1016/j.cell.2007.02.005.

Liteplo RG, Meek ME. 2003. Inhaled formaldehyde: Exposure estimation, hazard characterization, and exposure-response analysis. J Toxicol Environ Health B Crit Rev 6(1):85–114, PMID: 12587255, https://doi.org/10.1080/10937400306480.

Loyola A, Bonaldi T, Roche D, Imhof A, Almouzni G. 2006. PTMs on H3 variants before chromatin assembly potentiate their final epigenetic state. Mol Cell 24(2):309–316, PMID: 17052464, https://doi.org/10.1016/j.molcel.2006.08.019.

Lu K, Boysen G, Gao L, Collins LB, Swenberg JA. 2008. Formaldehyde-induced histone modifications *in vitro*. Chem Res Toxicol 21(8):1586–1593, PMID: 18656964, https://doi.org/10.1021/tx8000576.

Lu K, Collins LB, Ru H, Bermudez E, Swenberg JA. 2010. Distribution of DNA adducts caused by inhaled formaldehyde is consistent with induction of nasal carcinoma but not leukemia. Toxicol Sci 116(2):441–451, PMID: 20176625, https://doi.org/10.1093/toxsci/kfq061.

Lu K, Moeller B, Doyle-Eisele M, McDonald J, Swenberg JA. 2011. Molecular dosimetry of N^2-hydroxymethyl-dG DNA adducts in rats exposed to formaldehyde. Chem Res Toxicol 24(2):159–161, PMID: 21155545, https://doi.org/10.1021/tx1003886.

Marsh GM, Youk AO, Buchanich JM, Erdal S, Esmen NA. 2007. Work in the metal industry and nasopharyngeal cancer mortality among formaldehyde-exposed workers. Regul Toxicol Pharmacol 48(3):308–319, PMID: 17544557, https://doi.org/10.1016/j.yrtph.2007.04.006.

Mathijs K, Brauers KJ, Jennen DG, Lizarraga D, Kleinjans JC, van Delft JH. 2010. Gene expression profiling in primary mouse hepatocytes discriminates true from false-positive genotoxic compounds. Mutagenesis 25(6):561–568, PMID: 20650930, https://doi.org/10.1093/mutage/geq040.

Moeller BC, Lu K, Doyle-Eisele M, McDonald J, Gigliotti A, Swenberg JA. 2011. Determination of N^2-hydroxymethyl-dG adducts in the nasal epithelium and bone marrow of nonhuman primates following $^{13}CD_2$-formaldehyde inhalation exposure. Chem Res Toxicol 24(2):162–164, PMID: 21222454, https://doi.org/10.1021/tx1004166.

Monticello TM, Morgan KT, Everitt JI, Popp JA. 1989. Effects of formaldehyde gas on the respiratory tract of rhesus monkeys. Pathology and cell proliferation. Am J Pathol 134(3):515–527, PMID: 2923182.

Monticello TM, Swenberg JA, Gross EA, Leininger JR, Kimbell JS, Seilkop S, et al. 1996. Correlation of regional and nonlinear formaldehyde-induced nasal cancer with proliferating populations of cells. Cancer Res 56(5):1012–1022, PMID: 8640755.

NTP (National Toxicology Program). 2011. Formaldehyde. NTP 12th report on carcinogens. Rep Carcinog 12:195–206.

Pfaffl MW. 2001. A new mathematical model for relative quantification in real-time RT-PCR. Nucleic Acids Res 29(9):e45, PMID: 11328886, https://doi.org/10.1093/nar/29.9.e45.

Prado F, Aguilera A. 2005. Partial depletion of histone H4 increases homologous recombination-mediated genetic instability. Mol Cell Biol 25(4):1526–1536, PMID: 15684401, https://doi.org/10.1128/MCB.25.4.1526-1536.2005.

Rager JE, Moeller BC, Doyle-Eisele M, Kracko D, Swenberg JA, Fry RC. 2013. Formaldehyde and epigenetic alterations: MicroRNA changes in the nasal epithelium of nonhuman primates. Environ Health Perspect 121(3):339–344, PMID: 23322811, https://doi.org/10.1289/ehp.1205582.

Rager JE, Smeester L, Jaspers I, Sexton KG, Fry RC. 2011. Epigenetic changes induced by air toxics: Formaldehyde exposure alters miRNA expression profiles in human lung cells. Environ Health Perspect 119(4):494–500, PMID: 21147603, https://doi.org/10.1289/ehp.1002614.

Ransom M, Dennehey BK, Tyler JK. 2010. Chaperoning histones during DNA replication and repair. Cell 140(2):183–195, PMID: 20141833, https://doi.org/10.1016/j.cell.2010.01.004.

Recio L, Sisk S, Pluta L, Bermudez E, Gross EA, Chen Z, et al. 1992. p53 mutations in formaldehyde-induced nasal squamous cell carcinomas in rats. Cancer Res 52(21):6113–6116, PMID: 1394239.

Rice JC, Allis CD. 2001. Histone methylation versus histone acetylation: New insights into epigenetic regulation. Curr Opin Cell Biol 13(3):263–273, PMID: 11343896.

Saunders MJ, Yeh E, Grunstein M, Bloom K. 1990. Nucleosome depletion alters the chromatin structure of *Saccharomyces cerevisiae* centromeres. Mol Cell Biol 10(11):5721–5727, PMID: 2233714, https://doi.org/10.1128/MCB.10.11.5721.

Savic V, Yin B, Maas NL, Bredemeyer AL, Carpenter AC, Helmink BA, et al. 2009. Formation of dynamic gamma-H2AX domains along broken DNA strands is distinctly regulated by ATM and MDC1 and dependent upon H2AX densities in chromatin. Mol Cell 34(3):298–310, PMID: 19450528, https://doi.org/10.1016/j.molcel.2009.04.012.

Schöpf B, Bregenhorn S, Quivy JP, Kadyrov FA, Almouzni G, Jiricny J. 2012. Interplay between mismatch repair and chromatin assembly. Proc Natl Acad Sci USA 109(6):1895–1900, PMID: 22232658, https://doi.org/10.1073/pnas.1106696109.

Soria G, Polo SE, Almouzni G. 2012. Prime, repair, restore: The active role of chromatin in the DNA damage response. Mol Cell 46(6):722–734, PMID: 22749398, https://doi.org/10.1016/j.molcel.2012.06.002.

Suzuki YJ, Carini M, Butterfield DA. 2010. Protein carbonylation. Antioxid Redox Signal 12(3):323–325, PMID: 19743917, https://doi.org/10.1089/ars.2009.2887.

Swenberg JA, Kerns WD, Mitchell RI, Gralla EJ, Pavkov KL. 1980. Induction of squamous cell carcinomas of the rat nasal cavity by inhalation exposure to formaldehyde vapor. Cancer Res 40(9):3398–3402, PMID: 7427950.

Swenberg JA, Lu K, Moeller BC, Gao L, Upton PB, Nakamura J, et al. 2011. Endogenous versus exogenous DNA adducts: Their role in carcinogenesis, epidemiology, and risk assessment. Toxicol Sci 120 (Suppl 1):S130–S145, PMID: 21163908, https://doi.org/10.1093/toxsci/kfq371.

Swenberg JA, Moeller BC, Lu K, Rager JE, Fry RC, Starr TB. 2013. Formaldehyde carcinogenicity research: 30 years and counting for mode of action, epidemiology, and cancer risk assessment. Toxicol Pathol 41(2):181–189, PMID: 23160431, https://doi.org/10.1177/0192623312466459.

Szenker E, Ray-Gallet D, Almouzni G. 2011. The double face of the histone variant H3.3. Cell Res 21(3):421–434, PMID: 21263457, https://doi.org/10.1038/cr.2011.14.

Taddei A, Maison C, Roche D, Almouzni G. 2001. Reversible disruption of pericentric heterochromatin and centromere function by inhibiting deacetylases. Nat Cell Biol 3(2):114–120, PMID: 11175742, https://doi.org/10.1038/35055010.

Taddei A, Roche D, Sibarita JB, Turner BM, Almouzni G. 1999. Duplication and maintenance of heterochromatin domains. J Cell Biol 147(6):1153–1166, PMID: 10601331, https://doi.org/10.1083/jcb.147.6.1153.

Thompson CA, Burcham PC. 2008. Protein alkylation, transcriptional responses and cytochrome c release during acrolein toxicity in A549 cells: Influence of nucleophilic culture media constituents. Toxicol In Vitro 22(4):844–853, PMID: 18282682, https://doi.org/10.1016/j.tiv.2007.12.018.

van Kesteren PC, Zwart PE, Pennings JL, Gottschalk WH, Kleinjans JC, van Delft JH, et al. 2011. Deregulation of cancer-related pathways in primary hepatocytes derived from DNA repair-deficient $Xpa^{-/-}p53^{+/-}$ mice upon exposure to benzo[*a*]pyrene. Toxicol Sci 123(1):123–132, PMID: 21715664, https://doi.org/10.1093/toxsci/kfr169.

Vaughan TL, Stewart PA, Teschke K, Lynch CF, Swanson GM, Lyon JL, et al. 2000. Occupational exposure to formaldehyde and wood dust and nasopharyngeal carcinoma. Occup Environ Med 57(6):376–384, PMID: 10810126, https://doi.org/10.1136/oem.57.6.376.

Walport LJ, Hopkinson RJ, Schofield CJ. 2012. Mechanisms of human histone and nucleic acid demethylases. Curr Opin Chem Biol 16(5–6):525–534, PMID: 23063108, https://doi.org/10.1016/j.cbpa.2012.09.015.

Wang HX, Li HC, Lv MQ, Zhou DX, Bai LZ, Du LZ, et al. 2015. Associations between occupation exposure to formaldehyde and semen quality, a primary study. Sci Rep 5:15874, PMID: 26515386, https://doi.org/10.1038/srep15874.

Wiśniewski JR, Zougman A, Mann M. 2008. N^{ε}-formylation of lysine is a widespread post-translational modification of nuclear proteins occurring at residues involved in regulation of chromatin function. Nucleic Acids Res 36(2):570–577, PMID: 18056081, https://doi.org/10.1093/nar/gkm1057.

Ye X, Adams PD. 2003. Coordination of S-phase events and genome stability. Cell Cycle 2(3):185–187, PMID: 12734419.

Zhang L, Freeman LE, Nakamura J, Hecht SS, Vandenberg JJ, Smith MT, et al. 2010a. Formaldehyde and leukemia: Epidemiology, potential mechanisms, and implications for risk assessment. Environ Mol Mutagen 51(3):181–191, PMID: 19790261, https://doi.org/10.1002/em.20534.

Zhang L, Tang X, Rothman N, Vermeulen R, Ji Z, Shen M, et al. 2010b. Occupational exposure to formaldehyde, hematotoxicity, and leukemia-specific chromosome changes in cultured myeloid progenitor cells. Cancer Epidemiol Biomarkers Prev 19(1):80–88, PMID: 20056626, https://doi.org/10.1158/1055-9965.EPI-09-0762.